


 Cite this: *RSC Adv.*, 2022, 12, 3662

# Efficient fabrication of ordered alumina through-hole membranes using a TiO<sub>2</sub> protective layer prepared by atomic layer deposition

 Takashi Yanagishita,  \* Haruka Itoh and Hideki Masuda

Ordered alumina through-hole membranes were obtained by a combination of the anodization of Al, formation of a TiO<sub>2</sub> protective layer, and subsequent etching. Two-layered anodic porous alumina materials composed of TiO<sub>2</sub>-coated and noncoated alumina were prepared by the combination of the anodization of Al and the formation of a TiO<sub>2</sub> protective layer by atomic layer deposition (ALD). The obtained two layers of anodic porous alumina have different solubilities because the TiO<sub>2</sub> thin layer formed by ALD acts as a protective layer that prevents the dissolution of the alumina layer during wet etching of the sample in an etchant. After the selective dissolution of the bottom layer of porous alumina without the TiO<sub>2</sub> layer, an ordered alumina through-hole membrane could be detached from the Al substrate. This process allows the repeated preparation of ordered alumina through-hole membranes from a single Al substrate. By this process, ordered alumina through-hole membranes with large interhole distances could also be obtained. The obtained alumina through-hole membrane can be used in various applications.

Received 14th December 2021

Accepted 24th January 2022

DOI: 10.1039/d1ra09044e

[rsc.li/rsc-advances](https://rsc.li/rsc-advances)

## Introduction

Through-hole membranes composed of uniform-size holes have attracted considerable interest due to their various applicabilities, such as in filters, sensors, and templates.<sup>1–5</sup> There have been many reports on the preparation of through-hole membranes of polymers, metals, and metal oxides.<sup>6–8</sup> Among them, the anodization of Al is an effective process for the preparation of through-hole membranes with precisely controlled geometrical structures, including hole size, interhole distance, and hole depth.<sup>9–13</sup> In this material, as the interhole distance has a linear relationship with anodization voltage (2.5 nm V<sup>-1</sup>), the interhole distance of anodic porous alumina can be controlled by adjusting the anodization voltage. The hole depth can also be controlled by adjusting the anodization time. Additionally, anodic porous alumina with an ordered nanohole array structure can be prepared under appropriate anodization conditions.<sup>2</sup> For the preparation of an alumina through-hole membrane, it is necessary to remove the Al by selective dissolution or detachment using appropriate treatment.<sup>14–16</sup> In our previous study, we showed a novel process, called two-layer anodization, for the preparation of alumina through-hole membranes.<sup>17–21</sup> In this process, a combination of the anodization of Al in a typical anodization electrolyte and the subsequent anodization in concentrated sulfuric acid to form an extremely soluble alumina layer, followed by the selective

dissolution of the second layer yields the alumina through-hole membranes. This process is based on the higher solubility of the second layer, which contains a large number of sulfate anions that allow the selective dissolution.<sup>21</sup> After the formation of the through-hole membranes by selective etching, the surface of the residual Al has an ordered array of concaves, which corresponds to the ordered arrangement of the holes of the first anodization layer. The subsequent anodization of the Al with an ordered concave array generates the anodic porous alumina with an ordered hole arrangement because concaves formed on the surface of the Al substrate act as initiation sites of hole development. Despite these advantageous points compared with the traditional preparation process of the alumina through-hole membrane, this process has an unavoidable problem: the difficulty of the preparation of the alumina through-hole membrane with a large interhole distance. This is because stable anodization at a high anodization voltage of over 300 V, which corresponds to the interhole distance of 750 nm, is difficult in concentrated sulfuric acid owing to breakdown accompanied by spark discharge. To overcome this problem, we developed a new process for the preparation of alumina through-hole membranes, which is based on selective etching using TiO<sub>2</sub> protective layers formed by atomic layer deposition (ALD). Through the investigation of the etching properties of a sample of anodic porous alumina with a TiO<sub>2</sub> layer formed by ALD, we found that the TiO<sub>2</sub> layer acts as a protective layer against the dissolution of the alumina layer during wet etching of the sample in an etchant. From this finding, we could realize the efficient preparation of through-hole membranes by using

Department of Applied Chemistry, Tokyo Metropolitan University, 1-1 Minamiosawa, Hachioji, Tokyo 192-0397, Japan. E-mail: yanagish@tmu.ac.jp



the difference in the solubilities of the two-layered sample composed of  $\text{TiO}_2$ -coated and noncoated alumina. In the report, we describe a process for the preparation of two-layered samples and the formation of alumina through-hole membranes by selective dissolution. In this process, two-layered anodic porous alumina was formed by two anodizations of Al under the same anodization conditions with the insertion of  $\text{TiO}_2$  formation by ALD. This process enables the preparation of the sample with interhole distances larger than 750 nm because anodization in concentrated sulfuric acid is unnecessary. In addition, this process enables the preparation of alumina through-hole membranes with precisely controlled hole sizes because the  $\text{TiO}_2$  protective layer prevents any change in the hole sizes during etching. Even by this process, the repeated use of the Al and the efficient preparation of the ordered porous alumina can be achieved. This is the first report on the efficient preparation of an ordered alumina through-hole

membrane with a large interhole distance. The obtained alumina through-hole membrane is expected to be applied to various functional devices requiring an ordered array of large through-holes, such as membrane filters for the isolation and analysis of small microplastics and DNA size separation devices.<sup>22,23</sup>

## Experimental

Fig. 1 shows a schematic drawing of the preparation process for the ordered alumina through-hole membrane. For the examination of the formation of two-layered anodic porous alumina with different solubilities, ordered anodic porous alumina with an interhole distance of 100 nm was prepared by the process reported previously and used as a starting structure.<sup>24</sup> Ordered hole arrangement of anodic porous alumina can be obtained by long-term anodization under appropriate anodizing conditions.

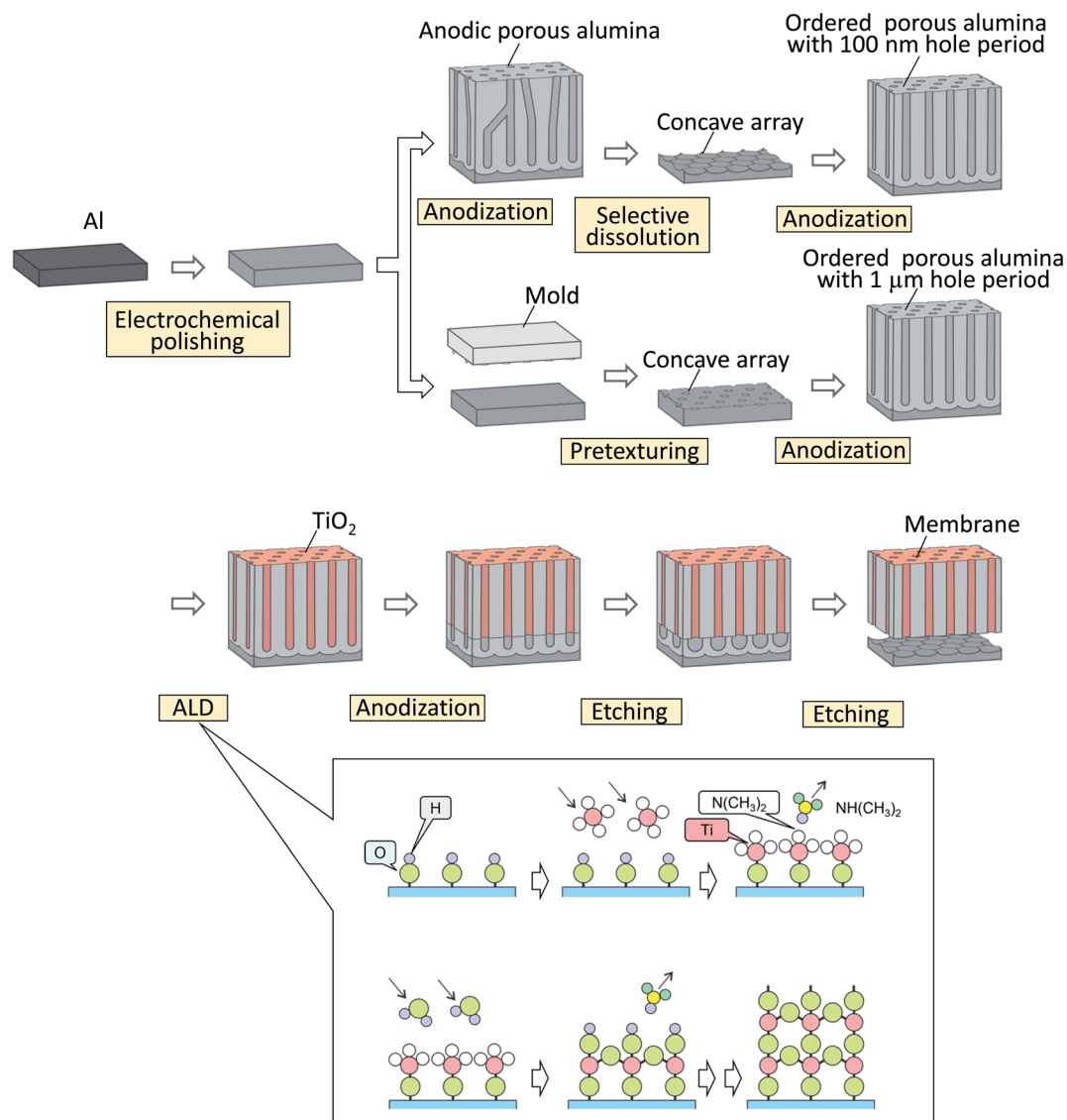


Fig. 1 Schematic diagram of preparation process of ordered alumina through-hole membrane.



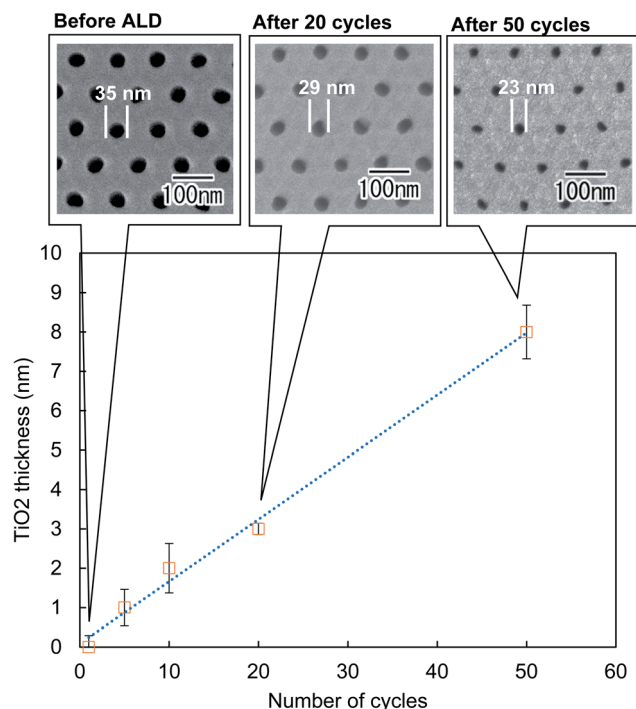


Fig. 2 Surface SEM images of anodic porous alumina before and after ALD, and relationship between TiO<sub>2</sub> thickness and number of ALD cycles.

This is because the degree of ordering in the hole arrangement increased with the depth of holes, which depends on the anodization time. For this reason, we adopt long anodization as the first step anodization. In this study, high purity Al sheet (99.99%) was used as the starting material. Prior to the anodization, the Al sheet was electrochemically polished using a mixture of perchloric acid and ethanol. The anodization of Al was performed in 0.3 M oxalic acid at 17 °C under a constant voltage of 40 V for 17 h to form the self-ordered hole arrangement at the bottom of anodic porous alumina. After the anodization, the oxide layer was dissolved selectively in a mixture of 1.8 wt% chromic acid and 6 wt% phosphoric acid of 50 °C for 3 h to obtain an Al substrate with an ordered concave array. The pretextured Al substrate was anodized again under the same conditions to form the ordered anodic porous alumina.

A TiO<sub>2</sub> thin layer was deposited on the surface of the obtained anodic porous alumina using ALD equipment, SAL3000Plus (SUGA Co., Japan).<sup>25</sup> For the ALD of TiO<sub>2</sub>, tetrakis(dimethylamido)titanium(IV) (TDMAT, Japan Advanced Chemicals, Japan) and distilled water were used as precursors. The chamber in which the sample was set was decompressed to 10 Pa and heated at 190 °C. One ALD cycle comprised a 250 ms injection of TDMAT into the chamber, a 750 s exposure of TDMAT, a 210 s N<sub>2</sub> purge, a 1000 ms injection of H<sub>2</sub>O in the chamber, a 210 s exposure of H<sub>2</sub>O, and a 210 s N<sub>2</sub> purge. This ALD cycle was repeated the desired number of times. After the ALD of TiO<sub>2</sub>, the two-layered anodic porous alumina with different solubilities was formed by the anodization of the sample in 0.3 M oxalic acid of 17 °C at 40 V.

The alumina through-hole membrane was obtained by selective dissolution of the lower part of the sample in a mixture of 1.8 wt% chromic acid and 6 wt% phosphoric acid of 50 °C for 15 min. After the etching treatment, the membrane could be detached easily because the alumina membrane was completely separated from the residual Al substrate by etching.

In the present work, the ordered anodic porous alumina with an interhole distance of 1 μm was prepared by the pretexturing process of Al reported previously.<sup>18</sup> Ordered anodic porous alumina with an interhole distance of 1 μm can also be prepared by long anodization in the appropriate condition. However, in order to obtain a highly ordered hole arrangement, first-step anodization exceeding 50 hours is required. Using the pretexturing process of Al, it is not possible to obtain large-area samples, but ordered anodic porous alumina with an inter hole distance of 1 μm can be easily prepared in a short time. Prior to the anodization, the Al substrate was pretextured using a Ni mold with an ordered convex array with a period of 1 μm to form a shallow concave array on the surface of Al. The pretextured Al was anodized in a mixture of 0.2 M citric acid and 2 mM phosphoric acid at 16 °C under a constant voltage of 400 V for 2 h.<sup>26</sup> The preparation of the ordered alumina through-hole membrane with an interhole distance of 1 μm was carried out by the same process as for an alumina membrane with an interhole distance of 100 nm. The obtained sample was observed by scanning electron microscopy (SEM; JSM-7500F, JEOL).

## Results and discussion

Fig. 2 shows the relationship between the number of ALD cycles and the thickness of the TiO<sub>2</sub> layer. The thickness of TiO<sub>2</sub> was estimated from the change in 1000 hole sizes of anodic porous alumina with an interhole distance of 100 nm after ALD. The thickness of the TiO<sub>2</sub> thin layer was increased with increasing number of ALD cycles, as shown in Fig. 2. From the investigation shown in Fig. 2, we confirmed that the thickness of TiO<sub>2</sub> and the number of ALD cycles have a linear relationship. Under the present ALD conditions, the growth rate of the TiO<sub>2</sub> layer was 0.16 nm per cycle.

Fig. 3(a) shows the cross-sectional SEM image of anodic porous alumina with an interhole distance of 100 nm after 10 ALD cycles of TiO<sub>2</sub>. An ordered hole array structure composed of uniform-size cylindrical holes was maintained even after ALD. Fig. 3(b) shows the cross-sectional SEM image of the sample after ALD and subsequent anodization. To facilitate SEM observation, the hole size of the first anodized layer was widened by etching in phosphoric acid before ALD of TiO<sub>2</sub>. In the SEM image, the two-layer hole array structure with different hole sizes was observed. This means that anodic porous alumina could be formed underneath the anodic porous alumina coated with the TiO<sub>2</sub> layer by the subsequent anodization of the sample. Fig. 3(c) shows the current density–time curves for samples having TiO<sub>2</sub> layers formed by different numbers of ALD cycles were anodized in 0.3 M oxalic acid at 40 V. In all samples, an increase in current density was observed during anodization. This indicates that the anodization of the



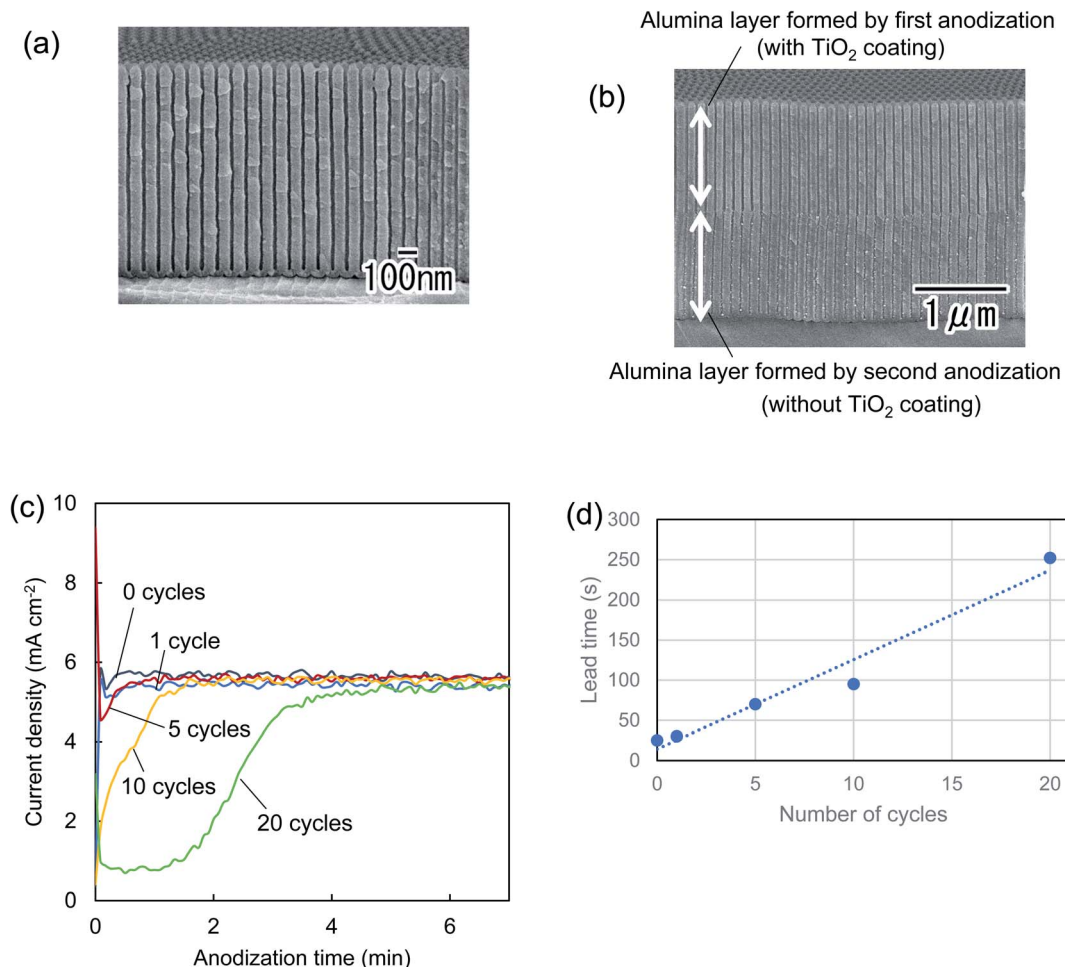


Fig. 3 (a) Cross-sectional SEM image of ordered anodic porous alumina after ALD of TiO<sub>2</sub>. (b) Cross-sectional SEM image of two-layered ordered anodic porous alumina after anodization. (c) Current density–time curves of TiO<sub>2</sub>-coated samples during anodization in 0.3 M oxalic acid at 40 V. (d) Relationship between number of ALD cycles and lead time of anodization.

samples proceeded even when the sample was treated with 20 ALD cycles. However, the lead time until the anodization current density increased lengthened with increasing number

of ALD cycles. This is because the growth of anodic porous alumina was prevented by the TiO<sub>2</sub> thin layer formed at the bottom of holes, and the growth suppression effect increased

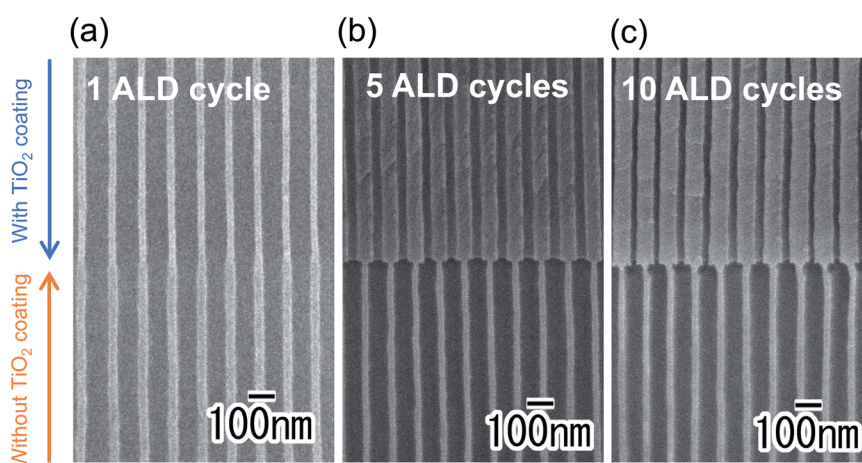


Fig. 4 Two-layered anodic porous alumina after etching. Numbers of ALD cycles of TiO<sub>2</sub> were (a) 1, (b) 5, and (c) 10.



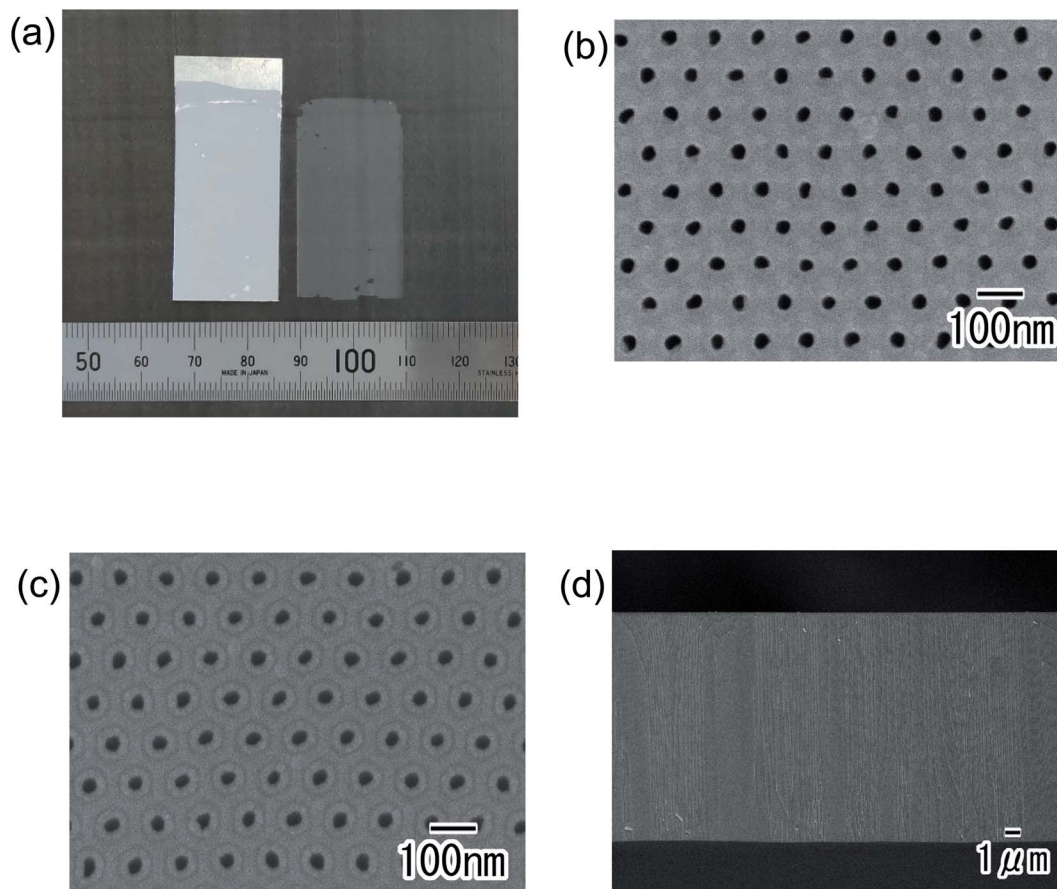


Fig. 5 (a) Photograph of detached alumina through-hole membrane and residual Al substrate. SEM images of the alumina through-hole membrane (b) top surface, (c) back surface, and (d) cross-sectional views. The thickness of the membrane was 15  $\mu\text{m}$ .

depending on the thickness of  $\text{TiO}_2$ . Fig. 3(d) shows the relationship between the number of ALD and lead time until the anodization current density reaches a steady-state value. This result indicates that the number of ALD and lead time have a leaner relationship. The progress of anodization after ALD was inhibited as the film thickness of the  $\text{TiO}_2$  layer formed at the bottom of the holes increased.

Fig. 4 shows SEM images of two-layered samples prepared by (a) 1, (b) 5, and (c) 10 ADL cycles after wet etching in a mixture of chromic acid and phosphoric acid for 5 min. In the case of the sample coated with  $\text{TiO}_2$  by 1 ALD cycle, shown in Fig. 4(a), it was observed that the hole diameter was widened at both the upper and lower parts. On the other hand, in the samples coated with  $\text{TiO}_2$  by over 5 ALD cycles, the holes were widened at the lower part of the anodic porous alumina without the  $\text{TiO}_2$  coating. This means that the  $\text{TiO}_2$  thin layer formed by over 5 ALD cycles, where the thickness of the  $\text{TiO}_2$  layer is *ca.* 1 nm, acts as a protective layer during etching. In the case of the sample treated with 5 ALD cycles without the injection of TDMAT, it was observed that the hole size was widened by etching treatment. This indicates that alumina dissolution is inhibited by the formation of a  $\text{TiO}_2$  thin layer through ALD rather than the crystallization of alumina through heat treatment. Since  $\text{TiO}_2$  is not dissolved by etching with phosphoric

acid, it can be assumed that a sparse coating layer was formed by 1 ALD cycle deposition. Therefore, it is thought that the etching of alumina proceeded from the part that could not be coated with  $\text{TiO}_2$ . On the other hand, in the samples that had

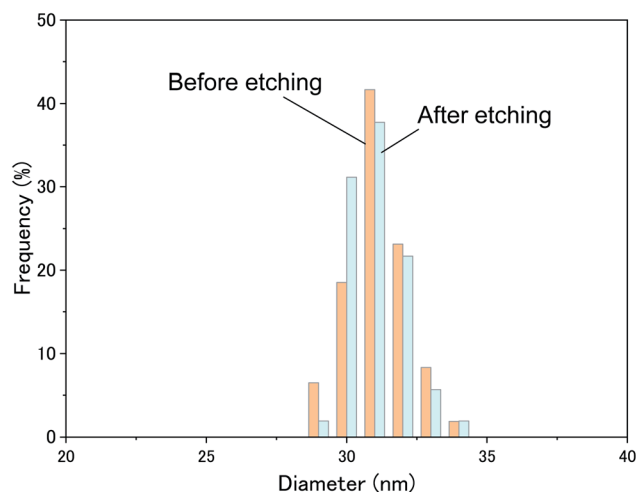


Fig. 6 Hole diameter histograms of the anodic porous alumina before and after etching treatment to obtain the through-hole membrane.



undergone ALD treatment more than 5 cycles, no change in hole diameter was observed before and after etching because the dense  $\text{TiO}_2$  layer formed on the inner wall of the pores functioned as an etching suppression layer. From these results, we concluded that two-layered anodic porous alumina with different solubilities could be obtained by the combination of anodization and ALD of  $\text{TiO}_2$ .

Fig. 5 shows the ordered alumina through-hole membrane obtained by the present process. Fig. 5(a) shows the detached membrane and the residual Al substrate. From this image, we observed that an alumina membrane without any cracks was detached from the Al substrate. The top surface, back surface, and cross-sectional SEM images shown in Fig. 5(b)–(d) indicate

that the uniform-size cylindrical through-holes were arranged hexagonally with an interhole distance of 100 nm. The thickness of the obtained membrane shown in Fig. 5 was 14  $\mu\text{m}$ .

Fig. 6 shows hole diameter histograms of the anodic porous alumina before and after etching treatment to obtain the through-hole membrane. For the measurement of hole diameters from SEM images, size distribution analysis software (MacView, Mountech Co., Japan) was used. From the obtained hole size distributions, it was confirmed that the average hole diameter of the sample before and after etching was 31 nm both before and after etching. This result indicates that the  $\text{TiO}_2$  thin layer formed on the anodic porous alumina prevents the dissolution of the alumina layer during the detachment of the

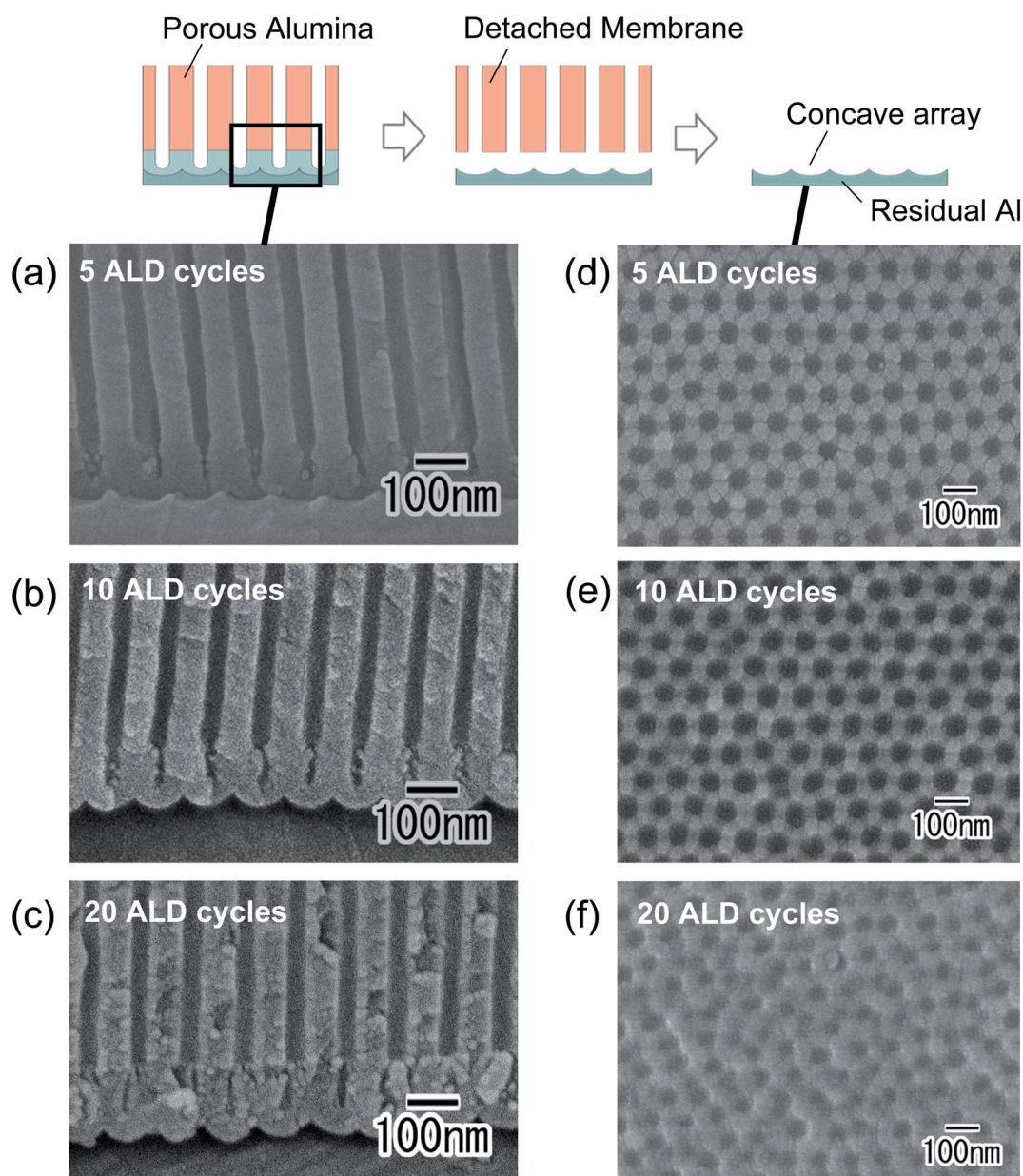


Fig. 7 Cross-sectional SEM images of samples after (a) 5, (b) 10, and (c) 20 ALD cycles of  $\text{TiO}_2$  and subsequent anodization. Surface SEM images of residual Al after detaching membranes. Numbers of ALD cycles before detaching membranes were (d) 5, (e) 10, and (f) 20.



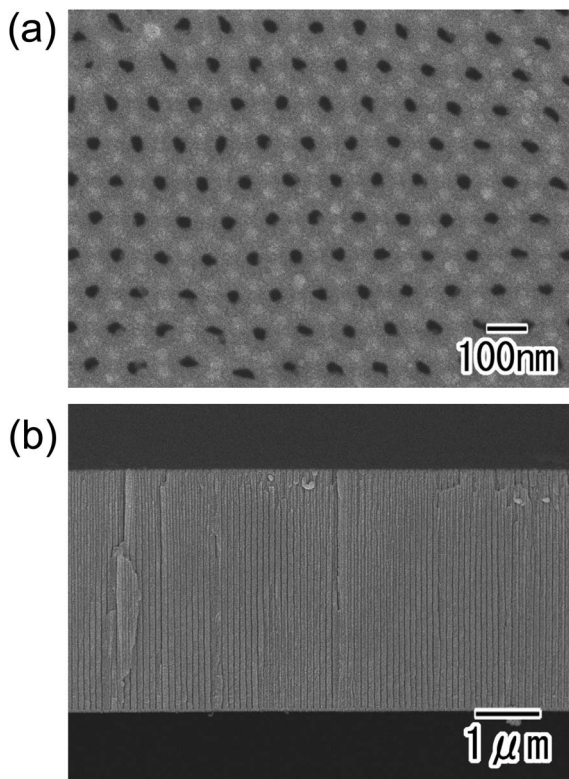


Fig. 8 SEM images of ordered alumina through-hole membrane obtained by four repetitions of our process: (a) surface and (b) cross-sectional views. The hole diameter and thickness of the membrane were 29 nm and 4  $\mu\text{m}$ , respectively.

membrane by etching. In other words, our process allows the preparation of ordered alumina through-hole membranes with precisely controlled hole diameters.

After the detachment of the alumina membrane, the residual Al could again be anodized. If an ordered concave array, which corresponds to the hole arrangement of the bottom of the membrane, can be maintained on the surface of the residual Al, the subsequent anodization of the residual Al generates an ordered anodic porous alumina because each concave acts as a starting point of hole development. Fig. 7 shows the results of the investigation of the effect of the ALD cycle number on the hole arrangement of anodic porous alumina obtained by anodization after ALD. After (a) 5, (b) 10, and (c) 20 ALD cycles of  $\text{TiO}_2$ , a second anodized oxide layer of 1  $\mu\text{m}$  thickness was formed by the subsequent anodization. Fig. 7(a)–(c) show cross-sectional SEM images of the bottom of anodic porous alumina after ALD of  $\text{TiO}_2$  and subsequent anodization. From the SEM observation, it was observed that up to 10 ALD cycles, a single hole was formed at the bottom of each hole. On the other hand, in the case of a sample coated with  $\text{TiO}_2$  by 20 ALD cycles, two or three holes were formed at the bottom of some holes. This means that the thickness of  $\text{TiO}_2$  affects the growth of holes during anodization. As shown in Fig. 3(c), the progress of anodization after ALD was inhibited as the film thickness of the  $\text{TiO}_2$  layer formed at the bottom of the holes increased. This is because the  $\text{TiO}_2$  layer is chemically stable in oxalic acid

electrolyte used for the anodization. Therefore, in a sample with thick  $\text{TiO}_2$  deposits, hole growth from the hole center of the first porous layer is prevented during anodization after ALD, and hole arrangement becomes disordered. Fig. 7(d)–(f) show surface SEM images of residual Al after removing the alumina layer. The ordered arranged arrays of concaves were observed at the samples prepared with 5 and 10 ALD cycles, as shown in Fig. 7(d) and (e). However, in the sample prepared with 20 ALD cycles, a disordered concave array was observed on the surface of residual Al. This result shows a good correspondence with the cross-sectional SEM image shown in Fig. 7(c). From these results, we concluded that it is possible to maintain the ordered hole arrangement during anodization after ALD of  $\text{TiO}_2$  by adjusting the number of ALD cycles.

Fig. 8 shows SEM images of the ordered through-hole membrane obtained by four repetitions of our process. From the surface and cross-sectional SEM images shown in Fig. 8(a) and (b), an ordered through-hole array was observed. This indicates that our process allows the repeated preparation of ordered through-hole membranes using a single Al substrate.

Fig. 9 shows the results of applying our process to the preparation of ordered alumina through-hole membrane with a large interhole distance. Fig. 9(a) shows an ordered alumina through-hole membrane with an interhole distance of 1  $\mu\text{m}$  and the residual Al. Alumina membrane with a thickness of more than 10  $\mu\text{m}$  can be handled by tweezers. Fig. 9(a) shows a photograph taken by pinching the membrane with tweezers. In both cases, the interference color of an ordered structure was observed. This means that the detached alumina membrane has an ordered hole array structure, and the surface of residual Al also has an ordered concave array. Surface and cross-sectional images of the membrane shown in Fig. 9(b) and (c), respectively, indicate that uniform-size cylindrical through-holes are arranged ideally over the sample. The thickness of the sample shown in Fig. 9 was 18  $\mu\text{m}$ . Fig. 9(d) shows an oblique SEM image of a membrane obtained by five repetitions of our process. It was observed that the ordered hole arrangement of anodic porous alumina prepared by the pretexturing process using the mold was maintained even after five repetitions of our process. From this result, we concluded that our process enables the repeated preparation of ordered alumina through-hole membranes with a large interhole distance using a single Al substrate.

In our process, the thickness of the alumina membrane can be controlled by adjusting the anodization time before the ALD of  $\text{TiO}_2$ . Fig. 10 shows the ordered alumina through-hole membranes with different thicknesses. The thicknesses of the membranes were (a) 30, (b) 40, and (c) 55  $\mu\text{m}$ , respectively. In addition, the hole diameter of the membrane could also be controlled by adjusting the pore-widening time before the ALD of  $\text{TiO}_2$ .

In the case of an alumina through-hole membrane with large interhole distance, the regularity of hole arrangement has a considerable effect on the transparency of the membrane. Fig. 11 shows membranes with and without regularity. Both membranes were prepared under the same anodization conditions: an electrolyte of 0.2 M citric acid and 2 mM phosphoric



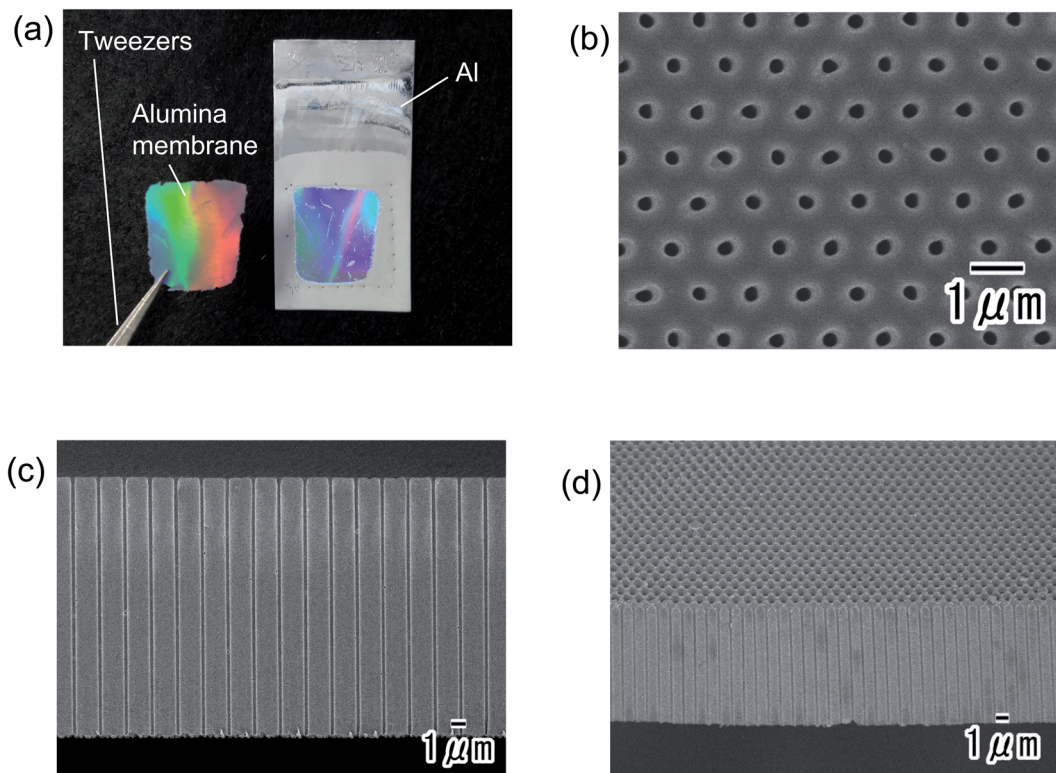


Fig. 9 (a) Photograph of detached alumina through-hole membrane with an interhole distance of  $1\ \mu\text{m}$  and residual Al. SEM images of the obtained alumina through-hole membrane with an interhole distance of  $1\ \mu\text{m}$ : (b) surface and (c) cross-sectional views. The hole diameter and thickness of the membrane were  $280\ \text{nm}$  and  $17\ \mu\text{m}$ , respectively. (d) SEM image of ordered alumina through-hole membrane obtained by five repetitions of our process. The thickness of the membrane was  $10\ \mu\text{m}$ .

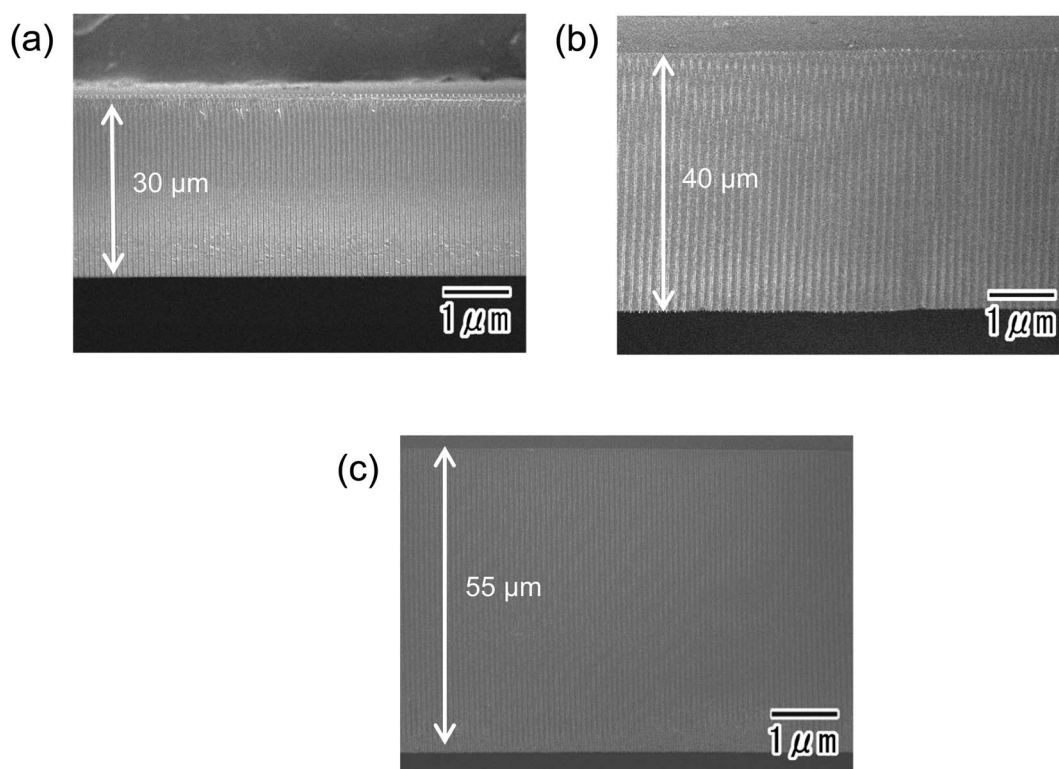


Fig. 10 SEM images of alumina through-hole membranes with thicknesses of (a)  $30\ \mu\text{m}$ , (b)  $40\ \mu\text{m}$ , and (c)  $55\ \mu\text{m}$ .



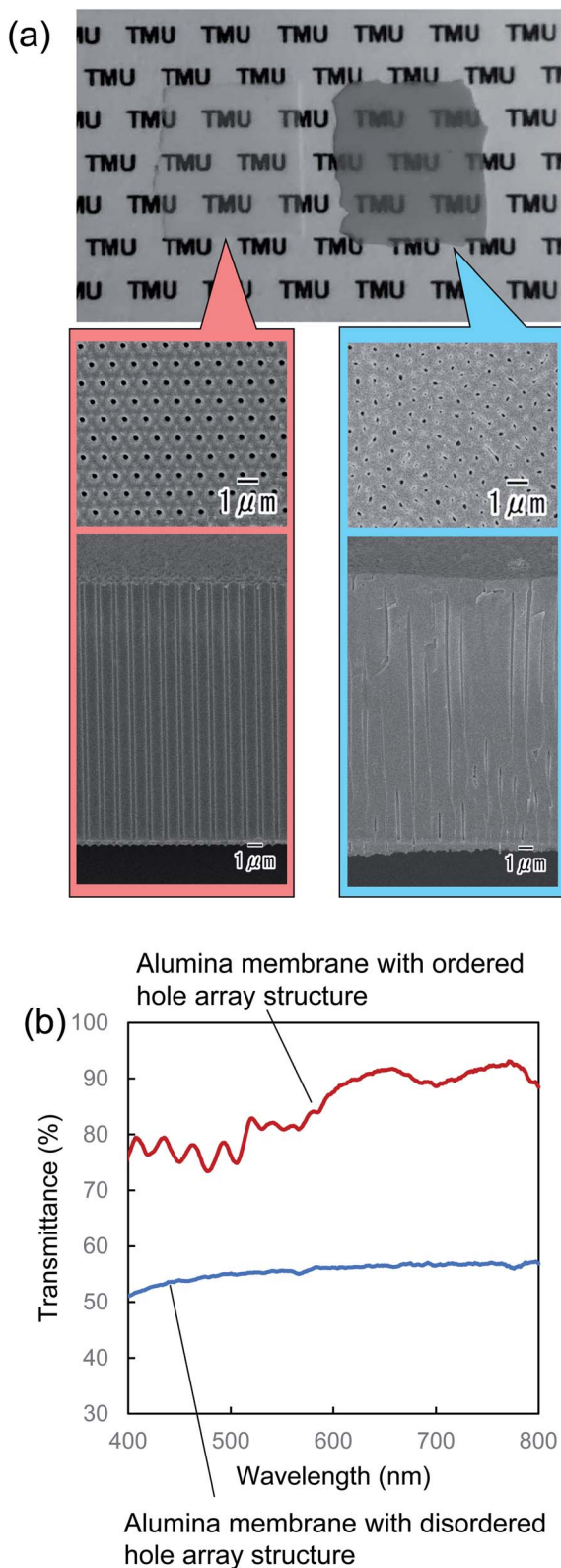


Fig. 11 (a) Photograph of alumina through-hole membranes with ordered and disordered hole arrangements. (b) Transmission spectra of the membranes. The thickness of both membranes was 17 μm.

acid at 400 V. The difference in the preparation of the samples is whether or not the concave array was formed by the pretexturing using a mold with an ordered convex array with a 1 μm period before anodization. The thickness of the membranes was 20 μm. From Fig. 11(a), it was observed that the characters on the back of the membrane with regularity were transparent, whereas those on the back of the membrane with irregularly arranged holes were obscured. This result originated from the difference in the regularity of the membranes. The membrane with regularity suppressed the diffraction of the incident lights and allowed satisfactory transparency. Fig. 11(b) shows transmission spectra of the membranes shown in Fig. 11(a). It can be observed that the membrane with regularity exhibits higher transmittance than the membrane without regularity. By our process, high-throughput preparation of transparent alumina through-hole membranes having large interhole distances and large holes can be achieved.

## Conclusion

Two-layered anodic porous alumina with different solubilities could be formed by the combination of the anodization of Al and the formation of a TiO<sub>2</sub> protective layer by ALD. The subsequent selective dissolution of the noncoated part of the two-layered anodic porous alumina generated the alumina through-hole membrane. This process enables the preparation of alumina through-hole membranes with large interholes by utilizing high applied voltages. When appropriate anodization conditions were applied, alumina through-hole membranes with ordered nanohole array structures could be obtained repeatedly using a single Al substrate. The obtained ordered alumina through-hole membrane with an interhole distance of 1 μm exhibited higher transparency than an alumina membrane without regularity. The sample obtained by our process can be expected to be used in various applications, such as transparent filters with large holes. In addition, the sample can be applied to a filter membrane having photocatalytic properties because the membrane obtained by this process has a TiO<sub>2</sub> layer on its surface.

## Author contributions

Takashi Yanagishita: conceptualization, methodology, investigation, writing – original draft. Haruka Itoh: investigation. Hideki Masuda: writing – review & editing.

## Conflicts of interest

There are no conflicts to declare.

## Acknowledgements

This research was supported by JSPS KAKENHI Grant Number JP20K05171.



## References

- 1 C. A. Huber, T. E. Huber, M. Sadoqi, J. A. Lubin, S. Manalis and C. B. Prater, *Science*, 1994, **263**, 800.
- 2 H. Masuda and K. Fukuda, *Science*, 1995, **268**, 1466.
- 3 E. M. I. M. Ekanayake, D. M. G. Preethichandra and K. Kaneto, *Biosens. Bioelectron.*, 2007, **23**, 107.
- 4 H. U. Osmanbeyoglu, T. B. Hur and H. K. Kim, *J. Membr. Sci.*, 2009, **343**, 1.
- 5 H. Zhao, C. Wang, R. Vellacheri, M. Zhou, Y. Xu, Q. Fu, M. Wu, F. Grote and Y. Lei, *Adv. Mater.*, 2014, **26**, 7654.
- 6 Y. Zhang, S. Yuan, X. Feng, H. Li, J. Zhou and B. Wang, *J. Am. Chem. Soc.*, 2016, **138**, 5785.
- 7 S. Ling, Z. Qin, W. Huang, S. Cao, D. L. Kaplan and M. J. Buehler, *Sci. Adv.*, 2017, **3**, e1601939.
- 8 N. Nasrollahi, V. Vatanpour, S. Aber and N. M. Mahmoodi, *Sep. Purif. Technol.*, 2018, **192**, 369.
- 9 J. Xue, Z. Zhou, Z. Wei, R. Su, J. Lai, J. Li, C. Li, T. Zhang and X. Wang, *Nat. Commun.*, 2015, **6**, 8906.
- 10 H. Robotjazi, S. M. Bahauddin, L. H. Macfarlan, S. Fu and I. Thomann, *Chem. Mater.*, 2016, **28**, 4546.
- 11 C. Zhang, Y. Lu, B. Zhao, Y. Hao and Y. Liu, *Appl. Surf. Sci.*, 2016, **377**, 167.
- 12 L. Ding, Y. Wei, Y. Wang, H. Chen, J. Caro and H. Wang, *Angew. Chem., Int. Ed.*, 2017, **56**, 1825.
- 13 Y. Yu, X. Wu, M. Zhao, Q. Ma, J. Chen, B. Chen, M. Sindoro, J. Yang, S. Han, Q. Lu and H. Zhang, *Angew. Chem., Int. Ed.*, 2017, **56**, 578.
- 14 Y. Li, G. S. Cheng and L. D. Zhang, *J. Mater. Res.*, 2000, **15**, 2305.
- 15 W. Lee, H. Han, A. Lotnyk, M. A. Schubert, S. Senz, M. Alexwe, D. Hense, S. Baik and U. Gösele, *Nat. Nanotechnol.*, 2008, **3**, 402.
- 16 J. J. Schneider, J. Engstler, K. P. Budna, C. Teichert and S. Franzka, *J. Inorg. Chem.*, 2005, **2005**, 2352.
- 17 T. Yanagishita and H. Masuda, *Electrochim. Acta*, 2015, **184**, 80.
- 18 T. Yanagishita, A. Kato and H. Masuda, *Jpn. J. Appl. Phys.*, 2017, **56**, 035202.
- 19 T. Yanagishita, A. Kato, T. Kondo and H. Masuda, *Jpn. J. Appl. Phys.*, 2020, **59**, 038002.
- 20 T. Yanagishita, M. Ozaki, R. Kawato, A. Kato, T. Kondo and H. Masuda, *J. Electrochem. Soc.*, 2020, **167**, 163502.
- 21 T. Yanagishita, A. Kato, T. Nakamura and H. Masuda, *ECS J. Solid State Sci. Technol.*, 2021, **10**, 013007.
- 22 M. Enfrin, J. Lee, P. Le-Clech and L. F. Dumée, *J. Membr. Sci.*, 2020, **1**, 117890.
- 23 L. Zhang, B. Majeed, L. Lagae, P. Peumans, C. V. Hoof and W. D. Malsche, *J. Chromatogr. A*, 2013, **1294**, 1.
- 24 H. Masuda and M. Satoh, *Jpn. J. Appl. Phys.*, 1996, **35**, L126.
- 25 T. Yanagishita, M. Otsuka, T. Takei, U. Seigo and H. Masuda, *Langmuir*, 2021, **37**, 8331.
- 26 T. Yanagishita, R. Moriyasu, T. Ishii and H. Masuda, *RSC Adv.*, 2021, **11**, 3777.

